Research article

# Worsening ozone air pollution with reduced $NO_x$ and VOCs in the Pearl River Delta region in autumn 2019: Implications for national control policy in China

Min Zhao [a,1], Yingnan Zhang [a,1], Chenglei Pei [b,c,d,e], Tianshu Chen [a], Jiangshan Mu [a], Yuhong Liu [a], Yujun Wang [d], Wenxing Wang [a], Likun Xue [a,f,*]

[a] Environment Research Institute, Shandong University, Qingdao, Shandong, 266237, China
[b] State Key Laboratory of Organic Geochemistry and Guangdong Key Laboratory of Environmental Protection and Resources Utilization, Guangzhou Institute of Geochemistry, Chinese Academy of Sciences, Guangzhou, Guangdong, 510640, China
[c] University of Chinese Academy of Sciences, Beijing, 100049, China
[d] Guangzhou Ecological and Environmental Monitoring Center of Guangdong Province, Guangzhou, Guangdong, 510060, China
[e] Guangdong Provincial Observation and Research Station for Climate Environment and Air Quality Change in the Pearl River Estuary, Guangzhou, Guangdong, 510275, China
[f] Collaborative Innovation Center for Climate Change, Nanjing, Jiangsu, 210023, China

## ARTICLE INFO

## ABSTRACT

Ozone ($O_3$) pollution has emerged as a major air quality issue in China. Here we emphasize the great challenges in controlling $O_3$ pollution by analyzing the recent experience of the Pearl River Delta (PRD) in southern China in reducing the autumn $O_3$ peaks. Despite significant reductions in the concentration of $O_3$ precursors, i.e., nitrogen oxides ($NO_x$) and volatile organic compounds (VOCs), regional $O_3$ pollution in the PRD was largely worse in autumn 2019 than in autumn 2018. We found that the supra-regional and regional background concentrations of $O_3$ increased significantly in the PRD in autumn 2019 due to increased concentrations of $O_3$ in the vast surrounding areas. We also observed slight increases in the concentrations of PRD-regionally and Guangzhou-locally produced $O_3$. A chemical box-model analysis confirmed a slight increase in the in-situ production of $O_3$ and revealed that increased biogenic VOCs (BVOCs) and decreased $NO_x$ levels negated the effect of significant decrease in the anthropogenic VOCs. Taken together, these aspects exacerbated $O_3$ pollution in the PRD region in autumn 2019 relative to autumn 2018. The findings from this study highlight the strong interactions of $O_3$ pollution over multiple regions and the need for collaborative inter-regional efforts to control $O_3$ pollution. The experience of PRD also underlines the key role of BVOCs and the importance of science-based strategies to decrease VOCs and $NO_x$.

## 1. Introduction

Ground-level ozone ($O_3$) air pollution has attracted great public concern due to its adverse effects on the economy, human health and plant growth (Ahmad et al., 2013; Li et al., 2018; Lippmann, 1991; Selin et al., 2009), and has become a widespread environmental problem in China in recent decades (Xue et al., 2014a,b). The implementation of the "Air Pollution Prevention and Control Action Plan" in the 2013–2017 period by the China State Council led to significant decreases in the concentrations of nitrogen oxides ($NO_x$, a major precursor of $O_3$) and

other routinely monitored pollutants, such as sulfur dioxide ($SO_2$), carbon monoxide (CO) and particulate matters (including $PM_{2.5}$ and $PM_{10}$) (He et al., 2017; Li et al., 2019b; Zeng et al., 2019). However, the concentration of $O_3$ is an exception, as levels of this pollutant have increased over many areas of China (Gaudel et al., 2018; Lu et al., 2020; Sun et al., 2016; Wang et al., 2017). As a result, $O_3$ pollution has been targeted as one of core challenges in air quality management in China. In particular, the management of emissions of volatile organic compounds (VOCs), another important class of $O_3$ precursors, will be attached more importance nationally in the near future.

The Pearl River Delta (PRD) region is one of the most developed regions in China, and has suffered from severe air pollution due to its rapid urbanization and industrialization. However, the PRD has controlled air pollution better than other major air pollution prevention regions in China. For example, the PRD has implemented stringent $PM_{2.5}$-control measures and, in 2015, became first of three air pollution hot spots (i.e., the PRD, the Beijing-Tianjin-Hebei region, and the Yangtze River Delta region) to meet the $PM_{2.5}$ Class II Chinese National Ambient Air Quality Standard (i.e., annual average of 35 μg/m$^3$), and has met this standard for the past 5 years. Despite these achievements, $O_3$ pollution has worsened in the PRD region, and $O_3$ has replaced $PM_{2.5}$ as the top air pollutant in the warm seasons (April–September) (China National Environmental Monitoring Station, 2017).

There are two challenges to mitigating $O_3$ pollution in the PRD and many other regions (Atkinson, 2000; Li et al., 2012; Sillman, 1999). The first challenge involves developing cost-effective measures to control $NO_x$ and VOC emissions, which is further complicated by the highly non-linear relationship between $O_3$ and its precursors ($NO_x$ and VOCs) (Tang et al., 2012). The second challenge involves understanding the dynamic transport of tropospheric $O_3$ pollution, as $O_3$ has a relatively long lifetime and can be transported to the areas adjacent from where it is formed. For $O_3$ pollution control, the understanding of dynamic transport over different scales and scientific control of different precursors are the primary focus.

To alleviate the severe $O_3$ pollution in the PRD, the Guangdong provincial government in 2017 established a series of regulations to strengthen control of VOC emissions (referred to as the "Autumn $O_3$ Peak Reduction Campaigns"). This series represents an extension of regulations to control VOC and $NO_x$ emissions that proposed reductions in the total anthropogenic emissions of VOCs and $NO_x$ by 18% and 3% from 2015 to 2020, respectively. During these campaigns, the government refined VOC emission management to target key industries and major anthropogenic sources. The entire PRD was involved, and Guangzhou, Shenzhen, Foshan, and Dongguan were listed as the demonstration cities for the campaign. The measurements confirmed significant decreases in anthropogenic $NO_x$ and VOC emissions during the "Autumn $O_3$ Peak Reduction Campaigns" in 2019 (see Section 3.1). However, $O_3$ pollution remains a problem in the PRD and the vast surrounding areas over southern China (Ozone Pollution Control Professional Committee, 2020). The experience of "Autumn $O_3$ Peak Reduction Campaigns" in autumn 2019 in the PRD region presents a unique opportunity to examine how $O_3$ pollution can worsen against the backdrops of significant reductions of $NO_x$ and VOCs in the PRD but rapid increase of $O_3$ concentrations in the surrounding areas.

In this study, the PRD and Guangzhou (the demonstration city and regional center in the PRD) were taken as examples to determine the reasons for increased $O_3$ pollution despite decreases in the concentrations of $NO_x$ and VOCs. The comprehensive measurement data during 2018–2019 were extracted for detailed analysis. First, we confirm that the emissions of $O_3$ precursors (mainly $NO_x$ and anthropogenic VOCs (AVOCs)) were better controlled but $O_3$ pollution still aggravated in Guangzhou and the PRD in autumn 2019 compared to autumn 2018. Then, we reveal that increases in the regional background concentrations of $O_3$ and local $O_3$ production led to worse $O_3$ pollution in Guangzhou, and conduct a series of sensitivity model tests to further quantify the effects of changes in $O_3$ precursors on local $O_3$ production. Finally, we determine the optimum AVOCs/$NO_x$ reduction ratios to effectively alleviate local $O_3$ formation and give recommendations for the future control of $O_3$ pollution.

## 2. Materials and methods

### 2.1. Measurement data

Two observational data sets were used for the analyses in this study. Briefly, ground-level $O_3$ concentration data were obtained from 1605 air-quality monitoring stations (AQMSs), which cover most areas of China, and the collected data reflect the inter-annual variations in national $O_3$ pollution (see Fig. 1(a)). The measurement data in autumn 2018 and autumn 2019 was extracted to evaluate the effectiveness of the "Autumn $O_3$ Peak Reduction Campaigns in 2019", which aimed to alleviate the severe $O_3$ pollution in autumn season, when $O_3$ exhibited maximum concentrations due to the polluted continental air masses coupled with dry and sunny weather conditions after the retreat of the summer marine air masses (Wang et al., 2009; Zheng et al., 2010). The $O_3$ inter-annual variation analysis was based on hourly and maximum daily 8-h average (MDA8) $O_3$ concentrations, and the $O_3$ non-attainment day was defined as a day when the MDA8 $O_3$ concentration exceeded the Chinese National Ambient Air Quality Standard, i.e., 75 ppbv (Class II). To eliminate the effect of nitric oxide (NO) titration, we also calculated the total oxidant ($O_x = O_3 + NO_2$) and MDA8 $O_x$ concentrations, and subjected them to similar analyses. In addition, the air-quality data obtained from 56 AQMSs in the PRD and 11 AQMSs in Guangzhou were analyzed to reveal the inter-annual variations over the study areas and to determine the regional background concentrations and locally produced concentrations of $O_3$.

Another data set was obtained from biennial comprehensive observations conducted in urban Guangzhou. Guangzhou is a megacity, the capital of Guangdong province, and the regional center of PRD (see Fig. 1 for the location of Guangzhou). Guangzhou plays a leading role in air pollution control in the PRD region, and was a demonstration city during the "Autumn $O_3$ Peak Reduction Campaigns". Therefore, changes in the concentrations of $NO_x$ and AVOCs over urban Guangzhou could well reflect the effects of $NO_x$ and AVOC control over the PRD. Field observations were conducted at an urban site (see Fig. 1(b) for its location) from January 1, 2018 to December 31, 2019, and data from autumn (September–November) 2018 and 2019 were extracted for the analysis. The comprehensive dataset comprises the concentrations of trace gases ($O_3$, $SO_2$, NO, $NO_2$, CO) and VOCs (57 compounds) and various meteorological parameters (temperature, relative humidity, and pressure). These data were subjected to a detailed chemical box modeling analysis to quantify the effects of changes in $O_3$ precursors on photochemical $O_3$ formation. Detailed information on the sampling site, measurement techniques, and quality assurance and control procedures are documented in the SI.

### 2.2. Estimation of regional background concentrations and local production of $O_3$

The Texas Commission on Environmental Quality (TCEQ) method was used to evaluate the contributions of background concentrations of $O_3$ over different scales to the observed levels of $O_3$ in Guangzhou and the PRD (Berlin et al., 2013; Kemball-Cook et al., 2009; Langford et al., 2009; Nielsen-Gammon et al., 2005). We modified the TCEQ method to contain three nested domains (Guangzhou, PRD, and outside the PRD), based on the following logic. The afore-mentioned 11 AQMSs in Guangzhou (56 AQMSs in the PRD) provide good coverage of Guangzhou (the PRD). At the local scale, as wind directions change, we can assume that at least one of the 11 AQMSs is always located upwind of Guangzhou. Therefore, the data collected at that site (or sites) are reasonably representative of the regional background concentrations of $O_3$ that are transported into Guangzhou, while other sites are additionally affected by their local photochemistry to varying extents. At a larger spatial (i.e., regional) scale, the 56 AQMSs within the PRD region can be used to estimate the supra-regional background concentrations of $O_3$ that are transported into the PRD and the concentrations of $O_3$ that are produced over the PRD.

Hence, the contributions of supra-regional (outside PRD) background, regionally (PRD) produced, and locally (Guangzhou) produced concentrations of $O_3$ to the observed concentrations of $O_3$ in Guangzhou can be estimated on a daily basis using the following equations (E1–E3), and then averaged for the entire autumn seasons of 2018 and 2019:
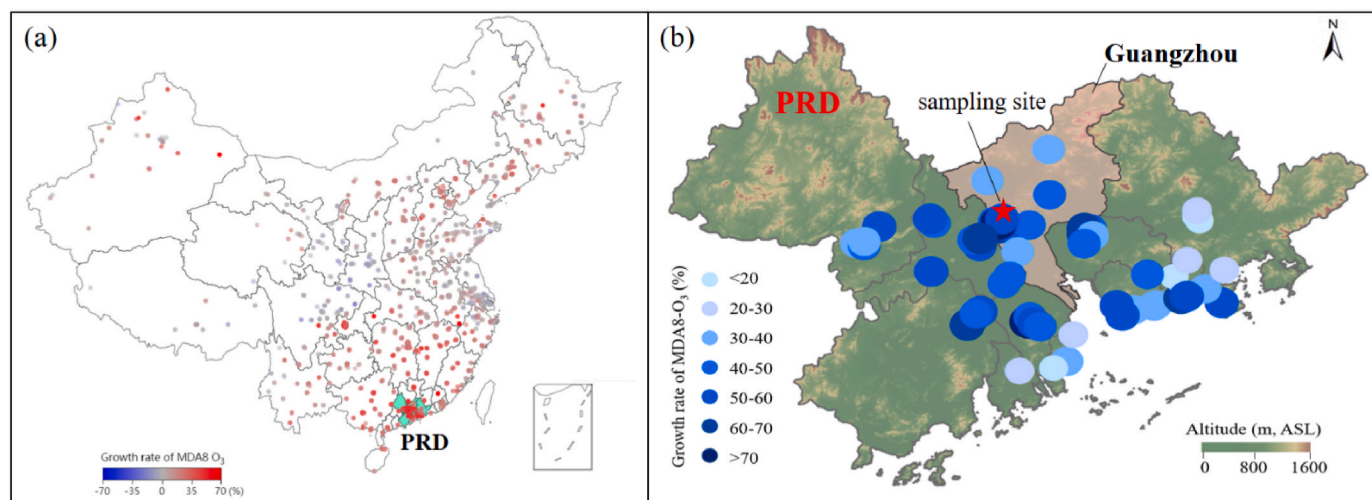
**Fig. 1.** The maps showing the inter-annual variations of autumn average maximum daily 8-h average ozone (MDA8 $O_3$) in (a) China and (b) the Pearl River Delta (PRD) region from 2018 to 2019. Also shown are the locations of (b) Guangzhou in the PRD and the sampling site in Guangzhou. The $O_3$ data were obtained from the Air-Quality Monitoring Stations from the public website of the China Ministry of Ecology and Environment.

$$C_{Supra-regional} = Min_{O_{X-PRD}} \tag{E1}$$

$$C_{Regional} = Min_{O_{X-Guangzhou}} - Min_{O_{X-PRD}} \tag{E2}$$

$$C_{Local} = Max_{O_{X-Guangzhou}} - Min_{O_{X-Guangzhou}} \tag{E3}$$

where $C_{Supra-regional}$, $C_{Regional}$, and $C_{Local}$ represent the contributions of the supra-regional background, regionally produced, and locally produced concentrations of $O_3$, respectively. $Min_{Ox}$ and $Max_{Ox}$ represent the lowest and the highest MDA8 $O_x$ concentrations recorded by the available AQMSs over a specific region (the PRD or Guangzhou), respectively.

Note that the local meteorology might lead to uncertainties in the TCEQ-estimated background $O_3$ concentrations (Berlin et al., 2013). To reduce the uncertainties, a least-squares linear regression analysis has been performed on TCEQ results, and the detailed information were documented in the SI.

### 2.3. Chemical box model

A chemical box model built on two different chemical mechanisms, namely the Master Chemical Mechanism (MCM v3.3.1; a near-explicit chemical mechanism) and the Regional Atmospheric Chemical Mechanism (RACM v2; a lumped chemical mechanism) (Goliff et al., 2013; Jenkin et al., 2003; Saunders et al., 2003), was adopted in the present study. Briefly, the MCM box model was used to quantify the net in-situ rate of $O_x$ production and to evaluate the effects of decreases in $O_3$ precursor concentrations on $O_3$ formation, and the RACM2 box model was used to establish $O_3$ isopleth diagrams that describe the nonlinear responses of $O_3$ concentrations to decreases in $O_3$ precursors. Our previous studies showed that both mechanisms agreed well with $O_3$ simulations (Zong et al., 2018), and the RACM2 was adopted for developing $O_3$ isopleth mainly due to its more efficient computation. Physical processes such as solar radiation, dry deposition, and planetary boundary layer evolution are also considered in the chemical box model. A detailed description of the model setup is provided elsewhere (Xue et al., 2016; Zhang et al., 2019).

Within the MCM model, the net rate of $O_x$ production was calculated as the difference between the rate of $O_x$ production ($P(O_x)$) and rate of $O_x$ loss ($L(O_x)$), which were quantified using Equations (S1)–(S2) in the SI. The observed $O_3$, CO, $SO_2$, NO, $NO_2$, and $C_2$–$C_{12}$ non-methane hydrocarbon (NMHC) concentrations, relative humidity, temperature, and pressure data were averaged or interpolated into a 1-h time resolution to constrain the model. Observed nitrous acid (HONO) concentration data were unavailable and therefore estimated by linear regression with $NO_2$ (see details in the SI). Sensitivity tests showed that a 1.5-fold change in the concentration of HONO would exert a relatively minor effect on the net rate of $O_x$ production, and would not change our major conclusions (see SI Fig. S2). The model was initiated at 00:00 local time (LT) on September 1, and the integration had a step of 1 h and duration of the entire autumn seasons (September–November) of 2018 and 2019. The model was pre-run for 3 days prior to each simulation to approach a steady state to stabilize the unconstrained species. A series of sensitivity tests were also conducted to evaluate the effects of changes in $O_3$ precursor concentrations on the net in-situ rate of $O_x$ production.

To establish the $O_3$ isopleth diagrams, the RACM2 box model was constrained in the base run by the autumn-average diurnal profiles of $SO_2$, CO, NO, $NO_2$ and $C_2$–$C_{12}$ NMHC concentrations, temperature, relative humidity, and pressure. Then, a series of emission-reduction simulations were conducted using X times (X = 0–1, with a bin of 0.05) the base concentrations of AVOCs and $NO_x$. To obtain a more reliable modeling result, the initial concentrations of oxygenated VOCs (OVOCs) and radicals (OH and $HO_2$) were prescribed according to the 2-day pre-run results. $O_3$ was initialized using the data observed at 06:00 h LT (the initial time of model integration), and its chemistry and concentrations were simulated using the constraints of other relevant species in the following integration. The model was initiated at 06:00 h LT, and the integration had a step of 1 h and duration of 24 h. The model-simulated maximum concentrations of $O_3$ under the base scenarios and 399 emission-reduction scenarios were extracted to describe the non-linear response of $O_3$ to decreases in the concentrations of $O_3$ precursors (similar to but slightly modified from the so-called EKMA plot).

## 3. Results and discussion

### 3.1. Variations in the autumn concentrations of $O_3$ and $O_3$ precursors between 2018 and 2019

We compared the concentrations of $NO_x$ and VOCs in urban Guangzhou between autumn 2018 and autumn 2019 to evaluate the effectiveness of air pollution control over the PRD region (shown in Fig. 2 (a) & (b)). Compared to 2018, $NO_x$ concentrations in 2019 were significantly lower (by 7%; $p < 0.01$) during the daytime (7:00–18:00 h LT) but slightly higher (by 4%; $p = 0.26$) during the nighttime (19:00–6:00 h LT). A similar inter-annual variation in the pattern of $NO_2$ concentrations was also revealed by data from 56 AQMSs over the PRD
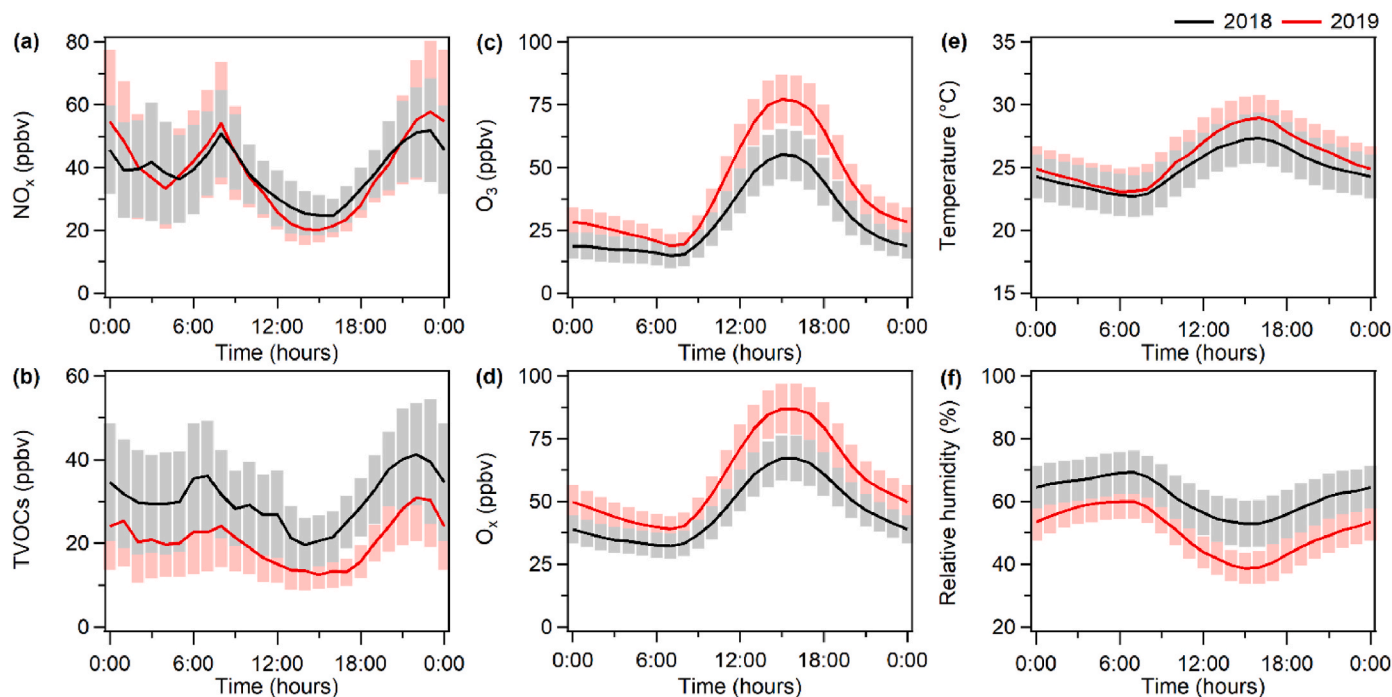
**Fig. 2.** Average diurnal variations in the concentrations of (a) nitrogen oxides ($NO_x$), (b) total volatile organic compounds (TVOCs), (c) ozone ($O_3$), and (d) $O_x$ ($O_x = O_3 + NO_2$), and meteorological parameters ((e) temperature and (f) relative humidity) in the Pearl River Delta (PRD) in autumn 2018 and autumn 2019. The error bars indicate a half-standard deviation of the mean. The concentrations of $O_3$ and $O_x$ were obtained from 56 air-quality monitoring stations in the PRD, the concentrations of $NO_x$ and VOCs, and the meteorological parameters (temperature and relative humidity) were measured at an urban site in Guangzhou, the capital city of Guangdong Province and the center of the PRD region.

(see SI Fig. S4). In comparison, remarkable decreases in both the daytime and nighttime concentrations of AVOCs were observed in 2019, compared with 2018. Specifically, the AVOC concentrations and their OH reactivities and $O_3$ formation potentials (OFP) decreased by 28%, 10%, and 20%, respectively (see Table. S1). Note that the OFP was calculated based on the localized maximum incremental reactivity (MIR) scales for Guangzhou (Zhang et al., 2021). A one-way analysis of variance revealed that all of these changes were statistically significant. A further inspection of the sub-group variations in AVOC concentrations revealed that the concentrations of alkenes (isoprene was excluded), aromatics, alkanes, and alkynes decreased by 28%, 27%, 29%, and 20%, respectively. In comparison, the concentrations of biogenic VOCs (BVOCs) (i.e., isoprene) significantly increased by 33%, which should be attributed to the higher leaf temperature and stronger photosynthetically active radiation (indicated by higher ambient temperatures) in autumn 2019 (Sabillon and Cremades, 2001; Chang et al., 2009). Similarly, decreases in AVOCs and increases in BVOCs were also observed in Shenzhen (another demonstration city of the "Autumn $O_3$ Peak Reduction Campaigns") during 2018–2019. Overall, the inter-annual variations in the concentrations of primary pollutants (especially AVOCs) demonstrate the success of the emission-reduction programs implemented in Guangzhou (as a demonstration city of the "Autumn $O_3$ Peak Reduction Campaigns") and the PRD, and provide an example for future VOC emission control programs in other regions of China.

Despite these significant decreases in the concentrations of AVOCs and $NO_x$, the concentrations of $O_3$ significantly increased in autumn 2019 compared with 2018 over most areas of the PRD, reaching a maximum increase of 70% (see Fig. 1(b)). As shown in Fig. 2, the concentrations of $O_3$ in the PRD increased by an average of 41% $\pm$ 21% ($p <$ 0.01) during the daytime and 44% $\pm$ 19% ($p <$ 0.01) during the nighttime. In addition, the concentrations of $O_x$ increased consistently and significantly during the daytime (by 29% $\pm$ 22%; $p <$ 0.01) and the nighttime (by 26% $\pm$ 20%; $p <$ 0.01). We also determined the inter-

annual variations in the number of $O_3$ non-attainment (exceedance) days on which the MDA8 $O_3$ exceeded 75 ppbv (see SI Fig. S5). In autumn 2019, there were a significant number of $O_3$ non-attainment days (41%; 37 days), compared to only a few such days in autumn 2018 (9%; 8 days). The higher concentrations of $O_3$ ($O_x$) and more non-attainment days indicate worse $O_3$ pollution in the PRD in autumn 2019 than in autumn 2018. The mechanism by which these distinct inter-annual variations in $O_3$ precursors (especially AVOCs) affected $O_3$ pollution remains unclear. It appears that the significant decreases in the $O_3$ precursor abundance in autumn 2019 did not work to alleviate $O_3$ pollution in the PRD, although the underlying cause remains unclear.

The inter-annual variations of other related factors were examined in Guangzhou, namely the $PM_{2.5}$ concentrations and meteorological parameters. Compared with autumn 2018, the $PM_{2.5}$ concentrations significantly increased in 2019 (by 10%; $p <$ 0.01, based on $PM_{2.5}$ data obtained from 11 AQMSs in Guangzhou). However, this increase can be excluded as a possible reason for the increased $O_3$ concentrations, due to the negative interactions between $O_3$ and $PM_{2.5}$ as reported by Li et al. (2019a). In addition, higher ambient temperature (by 4%; $p <$ 0.01) and lower relative humidity (by 18%; $p <$ 0.01) were recorded in autumn 2019 than in autumn 2018 (see Fig. 2); these meteorological conditions favor $O_3$ formation and may partly account for the worsened $O_3$ pollution in autumn 2019. The synoptic weather conditions during autumn 2019 certainly contributed to increases in $O_3$ pollution in the PRD and across southern China, compared with 2018, and significant increases in $O_3$ concentrations were indeed recorded at almost all of the AQMSs in these areas (see Fig. 1). However, these small or moderate variations in meteorological parameters should be insufficient to fully explain the significant increases in the $O_3$ concentration over the PRD in autumn 2019.

### 3.2. Increased regional-background and locally-produced $O_3$ in 2019

To identify the reasons for the significant increase in $O_3$

concentrations in autumn 2019, the contributions of background $O_3$ concentrations over different scales were quantified to the observed $O_3$ concentrations in Guangzhou and the PRD region (Fig. 3(a)). As shown, the regional background $O_x$ that was transported into Guangzhou comprised dominant contributions to the ambient concentrations of $O_x$ in Guangzhou in both 2018 (65% ± 12%) and 2019 (71% ± 9%). Similarly, the supra-regional background $O_x$ transported into the PRD made important contributions to the ambient concentrations of $O_x$ in the PRD in both 2018 (53% ± 13%) and 2019 (61% ± 12%). Compared with 2018, both the supra-regional and regional background $O_x$ concentrations increased in 2019 in terms of their absolute values (by 18 ppbv and 19 ppbv, respectively) and relative contributions (by 8% and 6%, respectively). This evidence directly demonstrates that the increasing supra-regional background $O_3$ concentrations contributed to the increased $O_3$ pollution over the PRD, which then indirectly contributed to the increased $O_3$ pollution over Guangzhou in 2019 via the inward transport of increased regional background $O_3$ from the PRD. These results are consistent with those reported by Xue et al. (2014b) and Yang et al. (2019), who identified increased regional background $O_3$ concentrations as a key contributor to the severe $O_3$ pollution in the PRD and Hong Kong in southern China. In addition, the increased contributions from regional background are consistent with the severe $O_3$ pollution over the vast area of eastern China, which has continually worsened in recent decades (Liu and Wang, 2020a, b; Lu et al., 2018). Driven by the synoptic conditions, the widespread exacerbation of $O_3$ pollution over southern China in autumn 2019 (Fig. 1) should account for increases in the supra-regional background concentrations of $O_3$ in the PRD region.

The inter-annual variations in the concentrations of regionally produced $O_3$ over the PRD and locally produced $O_3$ in Guangzhou were also presented. Compared with 2018, the regionally and locally produced $O_x$ concentrations didn't decrease and even slightly increased (by 1 ppbv) in 2019. In contrast, the concentrations of $O_3$ precursors, especially AVOCs, decreased significantly. It appears that the significant

reductions in AVOCs and $NO_x$ were inefficient for controlling local $O_3$ formation in autumn 2019. For comparison, the net in-situ rates of $O_x$ production during the entire autumn season in urban Guangzhou was calculated using the MCM box model (see Fig. 3(b)). The results obtained using two independent methods are generally consistent, as the model-calculated daytime rate of $O_x$ production in 2019 (13.80 ± 8.11 ppbv h$^{-1}$) was slightly higher than that in 2018 (13.52 ± 8.54 ppbv h$^{-1}$). Although the increases in the regionally and locally produced concentrations of $O_3$ are statistically insignificant and relatively small, compared with the changes in the supra-regional and regional background $O_3$ concentrations, it is important and unclear why significant decreases in the concentrations of $NO_x$ and AVOCs in urban Guangzhou (the PRD) led to increases or non-decreases in the locally (regionally) produced $O_3$ concentrations. Analogously, it is not apparent why the local photochemical production of $O_3$ did not decrease in response to the large reductions in $NO_x$ and AVOCs.

To investigate these aspects, a series of sensitivity modeling tests were conducted to quantify the effects of variations in the concentrations of individual major $O_3$ precursors (i.e., $NO_x$ and VOCs) on the in-situ $O_x$ production (see Fig. 4). The autumn 2018 was selected as a baseline and sensitivity tests were conducted using the target precursor concentrations constrained by the data in autumn 2019 while the other parameters were fixed. We found that the average daily maximum net rate of $O_x$ production was 21.1 ± 8.1 ppbv h$^{-1}$ in autumn 2018, and the effects of decreases of $NO_x$ and VOCs are clearly double-edged. Notably, the decrease in AVOCs in 2019 significantly lowered the daily maximum net rates of $O_x$ production (−4.57 ppbv h$^{-1}$ or -21.7%; $p < 0.01$). This confirms that controlling AVOC emissions can effectively reduce the local production of $O_3$. Further inspection shows that of the major AVOC groups, decrease in aromatic compounds led to the largest decrease in the daily maximum net rates of $O_x$ production (−2.37 ppbv h$^{-1}$ or -11.3%; $p < 0.05$), followed by decreases in alkanes (−2.32 ppbv h$^{-1}$ or -11.0%; $p < 0.05$) and alkenes (−0.48 ppbv h$^{-1}$ or -2.3%; $p = 0.69$). The relatively small effects of decreases in alkenes on the $O_x$ production relative to those of aromatics and alkanes are attributable to the higher concentrations of long-chain alkenes in 2019 than in 2018.

In comparison, a higher concentration level of isoprene led to greater local production of $O_3$, as demonstrated by a 1.24 ppbv h$^{-1}$ (5.9%) increase in the daily maximum net $O_x$ production rate in 2019 relative to
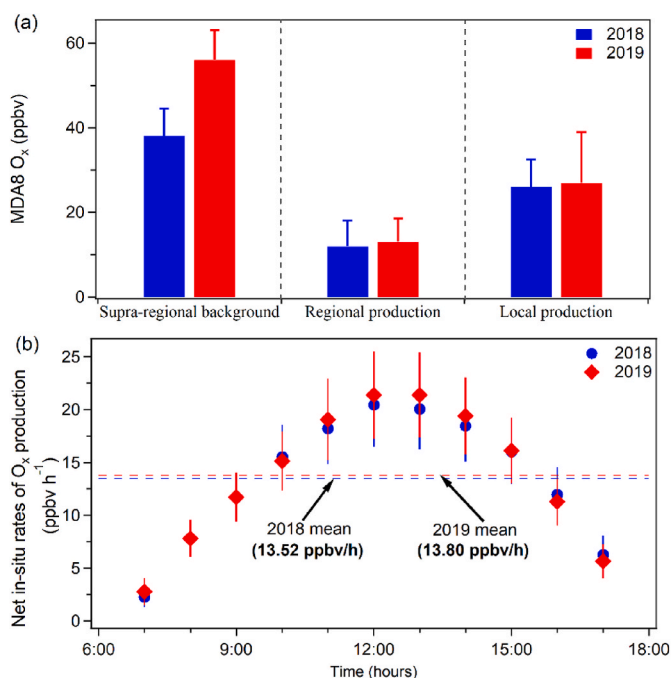
**Fig. 3.** (a) Contributions of the supra-regional background concentrations of $O_x$, Pearl River Delta (PRD)-regionally produced concentrations of $O_x$, and locally produced concentrations of $O_x$ to the observed concentrations of $O_x$ in Guangzhou; (b) Average diurnal variations in the modeled net in-situ rates of $O_x$ production at an urban site in Guangzhou. The error bars indicate a half-standard deviation of the mean.
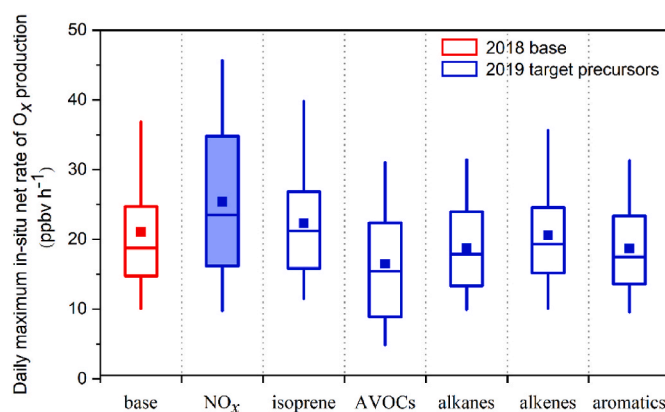
**Fig. 4.** Daily maximum net in-situ rates of $O_x$ production calculated using the Master Chemical Mechanism box model at an urban site in Guangzhou in autumn. The red box represents the base case results in 2018, and the blue boxes represent the sensitivity test results with the target precursor ($NO_x$, isoprene, AVOCs, alkanes, alkenes, and aromatics) concentrations constrained by observational data from 2019, while other parameters are fixed. The box plot provides the 5th, 25th, 50th, 75th, and 95th quantiles of the results. The solid bar represents "$NO_x$ disbenefits" (i.e., when decreased concentrations of $NO_x$ lead to increased concentrations of $O_3$). (For interpretation of the references to colour in this figure legend, the reader is referred to the Web version of this article.)

2018. Although $NO_x$ emissions were decreased (by 7% during the daytime) in 2019, the daily maximum net rate of $O_x$ production was significantly increased in 2019 (by 4.35 ppbv h$^{-1}$ or 20.7%; $p < 0.01$) due to a reduction in the NO titration effect. Evidently, the inadequate decrease in the emissions of $NO_x$ and increase in the emissions of BVOCs enhanced the in-situ $O_3$ production, which negated the benefits of the significant decrease in the emissions of AVOCs. For comparison, similar sensitivity studies were also conducted using autumn 2019 as a baseline, and the obtained results are generally consistent with those of the above sensitivity tests (see SI Fig. S6).

### 3.3. $O_3$-precursor relationships and implications for coordinated VOCs and $NO_x$ reduction

To establish future directions for the cost-effective control of $O_3$ pollution, a series of model scenarios was designed to establish the responses of $O_3$ concentrations to coordinated decreases in the emissions (concentrations) of AVOCs/$NO_x$ in urban Guangzhou (see Fig. 5). Urban Guangzhou is clearly under an $NO_x$-saturated and VOCs-limited $O_3$ formation regime in autumn, and therefore decreasing the concentrations of AVOCs is the most efficient approach for achieving short-term decreases in ambient $O_3$ levels. However, it is challenging to achieve long-term $O_3$ concentration objectives via a control strategy that is focused solely on decreasing AVOC concentrations, particularly as the PRD region has relatively intense BVOC emissions (see SI Fig. S7). Specifically, highly reactive BVOCs generally cannot be controlled by anthropogenic efforts, and increased concentrations of BVOCs could partly negate the effectiveness of significant decrease in AVOC emissions, thereby increasing the difficulty of controlling $O_3$.

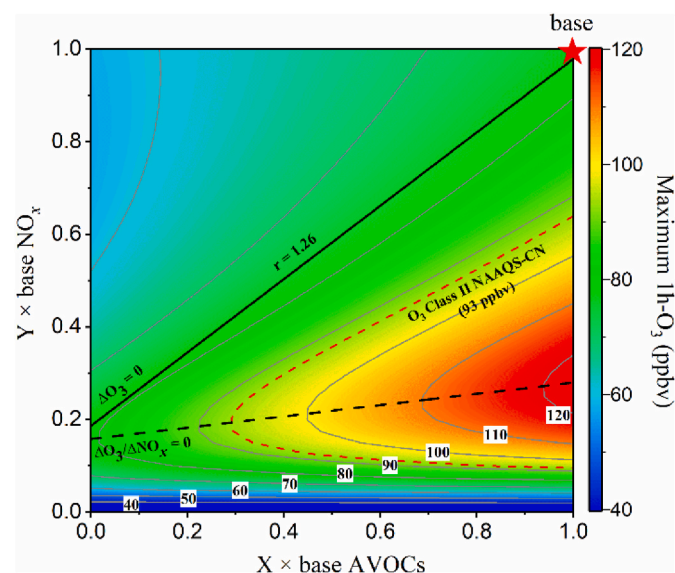To achieve the long-term control of $O_3$ pollution, the control policy

should target at transiting current $O_3$ formation regime from VOC-limited to $NO_x$-limited. For example, in urban Guangzhou, the desired $O_3$ attainment objective would be achieved if $NO_x$ emissions were decreased by $\geq$ 84% (see the black dashed line in Fig. 5); however, this would be challenging to achieve using the existing immature technologies. We also found that an AVOC/$NO_x$ concentration-reduction ratio >1.26 (the percentage-change in the concentration of AVOCs (ppbv)/ percentage-change in the concentration of $NO_x$ (ppbv); see the solid black line in Fig. 5) is a key requirement during a transition from high-to low-$NO_x$ concentration conditions, as it prevents an exacerbation of $O_3$ pollution, and this ratio value is comparable to those determined by previous studies (He et al., 2019; Ou et al., 2016; Sun et al., 2019). Overall, these results underscore that scientifically based decreases in AVOC/$NO_x$ emissions are required to prevent worsening $O_3$ pollution, and that large decreases in the emissions of $NO_x$ are fundamental to realizing long-term decreases in the concentrations of $O_3$.

The relative increment reactivity (RIR) for major $O_3$ precursor groups were also calculated, and the results are shown in Fig. 6. RIR is defined as the ratio of the percentage decrease in the simulated net rate of $O_x$ production to the percentage decrease in the concentration of the target precursor (10% in this case) (Cardelino and Chameides, 1995; Martien et al., 2003; Wang et al., 2018). A higher positive RIR value indicates that $O_3$ production is more sensitive to this precursor. AVOCs exhibited the highest positive RIRs (RIR = 1.22), and among AVOC groups, aromatics had the greatest influence (RIR = 0.70) on $O_3$ production. In contrast, the RIRs for the current $NO_x$ concentrations were highly negative (RIR = −1.02). This finding suggests that decreasing the emissions of aromatic compounds would most effectively decrease the local formation of $O_3$ in urban Guangzhou (the PRD), whereas decreasing the emissions of $NO_x$ by 10% would increase the formation of $O_3$.

### 3.4. Discussions: implications for future control of $O_3$ pollution in China

Current increases in the intensity and extent of $O_3$ air pollution in China have woken up the government and public, and the attainment of stipulated atmospheric $O_3$ concentrations has become a key target of air quality management in the upcoming 14th "Five-Year Plan" (2021–2025). Since 2013, the Chinese government has issued a series of emission control measures, such as "Air Pollution Prevention and Control Action Plan" (2013–2017) and "Three-Year Plan on Defending the Blue Sky" (2018–2021). As a consequence, the anthropogenic emissions of $SO_2$, $NO_2$ and CO have been reduced by 78%, 48% and 56% from 2013 to 2021, respectively, and the $PM_{2.5}$ concentrations have been reduced by 58% (Fig. S8), which were also demonstrated in previous
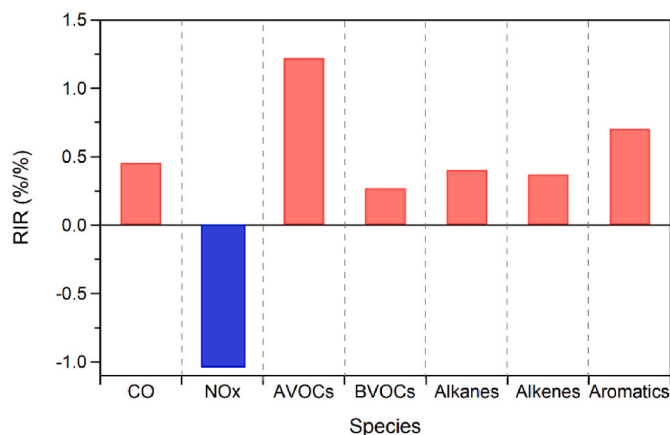


**Fig. 5.** Isopleths of the modeled maximum concentrations of ozone ($O_3$) as a function of X times the base concentrations of AVOCs and $NO_x$. The red pentagram represents the base (i.e., observed) concentrations of AVOCs and $NO_x$ in autumn 2019. The black solid line represents the fitting line for a base case with an AVOC/$NO_x$ reduction ratio of 1.26 [i.e., percentage change in concentration (ppbv)/percentage change in concentration (ppbv)], which exerts nearly zero effect on $O_3$ production (whereas the combined effects of an AVOC/$NO_x$ reduction ratio >1.26 (i.e., above the fitting line) would lead to decreased $O_3$ production). The black dashed line represents the line fitting that demonstrates the nearly zero effect of decreases in the concentrations of $NO_x$ on the production of $O_3$ (i.e., the boundary between the VOC-limited and mix-limited $O_3$ formation regime); the red dashed line represents the Class II Chinese National Ambient Air Quality Standard (NAAQS-CN) (i.e., 93 ppbv (hourly)). (For interpretation of the references to colour in this figure legend, the reader is referred to the Web version of this article.)



**Fig. 6.** The model-calculated relative increment reactivity (RIR) for ozone precursors (namely, CO, $NO_x$, AVOCs, and isoprene) and major AVOC groups (i. e., alkanes, alkenes, and aromatics).

studies (Cai et al., 2017; Maji et al., 2020; Zhao et al., 2021). However, these emission reduction measures have not been effective for mitigating $O_3$ pollution, as the $O_3$ concentrations still exhibited an upward trend in many regions of China (Lu et al., 2020; Wang et al., 2022). Reduction in $NO_x$ emission is indeed the correct way to control photochemical $O_3$ pollution. However, extensive evidence indicates that the current strategy for controlling and decreasing $NO_x$ emissions is insufficient for mitigating $O_3$ pollution, as $O_3$ formation persists in $NO_x$-saturated and VOC-limited regimes in a variety of urban areas (Sun et al., 2019). In comparison with efforts to control $NO_x$ emissions, efforts to VOC emissions have been largely lagged in China, due to the complexity of emission sources and a lack of control technologies. Hence, the AVOC-focused control strategy has been adopted by the government as the hope to control $O_3$ pollution in the future step. In this context, the experience of $O_3$ pollution control in the PRD region, as presented in this study, provides a valuable lesson for the entire area of eastern China, which is currently struggling with worsening regional $O_3$ air pollution. Thus, the key implications of the $O_3$ pollution control in the PRD are as follows.

First, science-based coordinated control of AVOC and $NO_x$ emissions is the key to lessen local $O_3$ production in short-term or medium-term stages. Under an $NO_x$-saturated $O_3$-formation regime, a small (or moderate) decrease in the concentrations of $NO_x$ may negate the effectiveness of large decreases in the concentrations of AVOCs. The optimum AVOC/$NO_x$ reduction ratio must therefore be regularly examined on a yearly (or seasonal) basis, and should be based on changes in synoptic weather conditions, progress in emission reduction, and the development of control technologies. Long-term $O_3$ attainment strategy will require large decreases in the emissions of $NO_x$, as this is the fundamental way to transform the current high-$NO_x$ environment to a low-$NO_x$ environment. Innovations in denitrification technology are highly needed to enable this transformation. Second, the emissions of BVOCs under unfavorable weather conditions are an important factor that perturbs attempts to control $O_3$ pollution, especially given the acceleration of afforestation and urban greening in recent decades in China. Given the high photochemical reactivity of BVOCs, a small increase in BVOCs may substantially influence the magnitude of the required decreases in emissions of AVOCs. Finally, it would be insufficient to resolve severe $O_3$ pollution by only local emission reductions in an individual region, as $O_3$ pollution is a regional environmental problem and can be transported over multiple regions. There is an urgent need for synchronous control on regional emissions over most areas of China towards national $O_3$ pollution mitigation, especially under unfavorable synoptic weather conditions.

## 4. Summary

We evaluated the effectiveness of the "Autumn $O_3$ Peak Reduction Campaign 2019" implemented in the PRD region, which aimed at mitigating $O_3$ pollution by largely cutting down anthropogenic emissions of VOCs and $NO_x$. This program was successful in reducing the ambient concentrations of AVOCs and $NO_x$, but failed to lessen regional $O_3$ pollution, which was even much worse in autumn 2019 compared to autumn 2018. Further inspections revealed that both the increased background and locally-produced $O_3$ contributed to the worsened $O_3$ pollution observed in the PRD in autumn 2019. At a large scale, the supra-regional and regional background $O_3$ concentrations significantly increased in the PRD due to the elevated $O_3$ concentrations from the vast surrounding areas. At a local scale, increased BVOCs and decreased $NO_x$ negated the effect of significant decreases in AVOCs on in-situ $O_3$ formation. The unsuccessful experience of the PRD in reducing autumn $O_3$ peaks highlights the currently existing challenges of $O_3$ pollution control in China, and demonstrates the importance of science-based AVOCs/$NO_x$ control strategy and synchronous control on regional emissions to the national $O_3$ pollution mitigation in China, which also has important implications for other countries suffering from serious $O_3$ air pollution.

## Author statement

**Min Zhao**[1]: Conceptualization, Formal analysis, Writing – original draft. **Yingnan Zhang**[1]: Conceptualization, Formal analysis, Writing – review & editing. **Chenglei Pei**: Investigation, Resources. **Tianshu Chen**: Methodology, Software. **Jiangshan Mu**: Methodology. **Yuhong Liu**: Methodology. **Yujun Wang**: Investigation. **Wenxing Wang**: Supervision, Resources. **Likun Xue**: Conceptualization, Funding acquisition, Project administration, Writing – review & editing.

## Declaration of competing interest

The authors declare that they have no known competing financial interests or personal relationships that could have appeared to influence the work reported in this paper.

## Data availability

Data will be made available on request.

## Appendix A. Supplementary data

Supplementary data to this article can be found online at https://doi.org/10.1016/j.jenvman.2022.116327.

## References

Ahmad, M.N., Buker, P., Khalid, S., Van den Berg, L., Shah, H.U., Wahid, A., Emberson, L., Power, S.A., Ashmore, M., 2013. Effects of ozone on crops in northwest Pakistan. Environ. Pollut. 174, 244–249.

Atkinson, R., 2000. Atmospheric chemistry of VOCs and $NO_x$. Atmos. Environ. 34, 2063–2101.

Berlin, S.R., Langford, A.O., Estes, M., Dong, M., Parrish, D.D., 2013. Magnitude, decadal changes, and impact of regional background ozone transported into the greater houston, Texas, area. Environ. Sci. Technol. 47, 13985–13992.

Cai, S., Wang, Y., Zhao, B., Wang, S., Chang, X., Hao, J., 2017. The impact of the "air pollution prevention and control action plan" on $PM_{2.5}$ concentrations in Jing-Jin-Ji region during 2012–2020. Sci. Total Environ. 580, 197–209.

Cardelino, C.A., Chameides, W.L., 1995. An observation-based model for analyzing ozone precursor relationships in the urban atmosphere. J. Air Waste Manag. Assoc. 45, 161–180.

Chang, K.H., Yu, J.Y., Chen, T.F., Lin, Y.P., 2009. Estimating Taiwan biogenic VOC emission: leaf energy balance consideration. Atmos. Environ. 43, 5092–5100.

China National Environmental Monitoring Station, 2017. Ambient Air Quality Report of 74 Cities in the First Half of 2017 (Beijing, China).

Gaudel, A., Cooper, O.R., Ancellet, G., Barret, B., Boynard, A., Burrows, J.P., Clerbaux, C., Coheur, P.F., Cuesta, J., Cuevas, E., Doniki, S., Dufour, G., Ebojie, F., Foret, G., Garcia, O., Granados-Munoz, M.J., Hannigan, J.W., Hase, F., Hassler, B., Huang, G., Hurtmans, D., Jaffe, D., Jones, N., Kalabokas, P., Kerridge, B., Kulawik, S., Latter, B., Leblanc, T., Le Flochmoen, E., Lin, W., Liu, J., Liu, X., Mahieu, E., McClure-Begley, A., Neu, J.L., Osman, M., Palm, M., Petetin, H., Petropavlovskikh, I., Querel, R., Rahpoe, N., Rozanov, A., Schultz, M.G., Schwab, J., Siddans, R., Smale, D., Steinbacher, M., Tanimoto, H., Tarasick, D.W., Thouret, V., Thompson, A.M., Trickl, T., Weatherhead, E., Wespes, C., Worden, H.M.,

Vigouroux, C., Xu, X., Zeng, G., Ziemke, J., 2018. Tropospheric Ozone Assessment Report: present-day distribution and trends of tropospheric ozone relevant to climate and global atmospheric chemistry model evaluation. Elementa-Science of the Anthropocene 6, 58.

Goliff, W.S., Stockwell, W.R., Lawson, C.V., 2013. The regional atmospheric chemistry mechanism, version 2. Atmos. Environ. 68, 174–185.

He, J.J., Gong, S.L., Yu, Y., Yu, L.J., Wu, L., Mao, H.J., Song, C.B., Zhao, S.P., Liu, H.L., Li, X.Y., Li, R.P., 2017. Air pollution characteristics and their relation to meteorological conditions during 2014-2015 in major Chinese cities. Environ. Pollut. 223, 484–496.

He, Z.R., Wang, X.M., Ling, Z.H., Zhao, J., Guo, H., Shao, M., Wang, Z., 2019. Contributions of different anthropogenic volatile organic compound sources to ozone formation at a receptor site in the Pearl River Delta region and its policy implications. Atmos. Chem. Phys. 19, 8801–8816.

Jenkin, M.E., Saunders, S.M., Wagner, V., Pilling, M.J., 2003. Protocol for the development of the Master Chemical Mechanism, MCM v3 (Part B): tropospheric degradation of aromatic volatile organic compounds. Atmos. Chem. Phys. 3, 181–193.

Kemball-Cook, S., Parrish, D., Ryerson, T., Nopmongcol, U., Johnson, J., Tai, E., Yarwood, G., 2009. Contributions of regional transport and local sources to ozone exceedances in Houston and Dallas: comparison of results from a photochemical grid model to aircraft and surface measurements. J. Geophys. Res. Atmos. 114, 14.

Langford, A.O., Senff, C.J., Banta, R.M., Hardesty, R.M., Alvarez, R.J., Sandberg, S.P., Darby, L.S., 2009. Regional and local background ozone in houston during Texas air quality study 2006. J. Geophys. Res. Atmos. 114, 12.

Li, K., Jacob, D.J., Liao, H., Shen, L., Zhang, Q., Bates, K.H., 2019a. Anthropogenic drivers of 2013-2017 trends in summer surface ozone in China. Proc. Natl. Acad. Sci. U.S.A. 116, 422–427.

Li, R., Wang, Z.Z., Cui, L.L., Fu, H.B., Zhang, L.W., Kong, L.D., Chen, W.D., Chen, J.M., 2019b. Air pollution characteristics in China during 2015-2016: spatiotemporal variations and key meteorological factors. Sci. Total Environ. 648, 902–915.

Li, Y., Lau, A.K.H., Fung, J.C.H., Zheng, J.Y., Zhong, L.J., Louie, P.K.K., 2012. Ozone source apportionment (OSAT) to differentiate local regional and super-regional source contributions in the Pearl River Delta region, China. J. Geophys. Res. Atmos. 117, 18.

Li, Y., Shang, Y., Zheng, C., Ma, Z., 2018. Estimated acute effects of ozone on mortality in a rural district of Beijing, China, 2005-2013: a time-stratified case-crossover study. Int. J. Environ. Res. Publ. Health 15.

Lippmann, M., 1991. Health effects of tropospheric ozone. Environ. Sci. Technol. 25, 1954–1962.

Liu, Y.M., Wang, T., 2020a. Worsening urban ozone pollution in China from 2013 to 2017-Part 1: the complex and varying roles of meteorology. Atmos. Chem. Phys. 20, 6305–6321.

Liu, Y.M., Wang, T., 2020b. Worsening urban ozone pollution in China from 2013 to 2017-Part 2: the effects of emission changes and implications for multi-pollutant control. Atmos. Chem. Phys. 20, 6323–6337.

Lu, X., Hong, J.Y., Zhang, L., Cooper, O.R., Schultz, M.G., Xu, X.B., Wang, T., Gao, M., Zhao, Y.H., Zhang, Y.H., 2018. Severe surface ozone pollution in China: a global perspective. Environ. Sci. Technol. Lett. 5, 487–494.

Lu, X., Zhang, L., Wang, X.L., Gao, M., Li, K., Zhang, Y.Z., Yue, X., Zhang, Y.H., 2020. Rapid increases in warm-season surface ozone and resulting health impact in China since 2013. Environ. Sci. Technol. Lett. 7, 240–247.

Maji, K.J., Li, V.O.K., Lam, J.C.K., 2020. Effects of China's current Air Pollution Prevention and Control Action Plan on air pollution patterns, health risks and mortalities in Beijing 2014–2018. Chemosphere 260, 127572.

Martien, P.T., Harley, R.A., Milford, J.B., Russell, A.G., 2003. Evaluation of incremental reactivity and its uncertainty in Southern California. Environ. Sci. Technol. 37, 1598–1608.

Nielsen-Gammon, J., Tobin, J., McNeel, A., Li, G., 2005. A Conceptual Model for Eight-Hour Ozone Exceedances in Houston, Texas Part I: Background Ozone Levels in Eastern Texas.

Ou, J.M., Yuan, Z.B., Zheng, J.Y., Huang, Z.J., Shao, M., Li, Z.K., Huang, X.B., Guo, H., Louie, P.K.K., 2016. Ambient ozone control in a photochemically active region: short term despiking or long-term attainment? Environ. Sci. Technol. 50, 5720–5728.

Ozone Pollution Control Professional Committee, 2020. The Blue Book of Atmospheric Ozone Pollution and Prevention in China. In: The 2nd China Seminar on Prevention and Control of Atmospheric Ozone Pollution (Nanjing, China).

Sabillon, D., Cremades, L.V., 2001. Diurnal and seasonal variation of monoterpene emission rates for two typical Mediterranean species (Pinus pinea and Quercus ilex)

from field measurements-relationship with temperature and PAR. Atmos. Environ. 35, 4419–4431.

Saunders, S.M., Jenkin, M.E., Derwent, R.G., Pilling, M.J., 2003. Protocol for the development of the Master Chemical Mechanism, MCM v3 (Part A): tropospheric degradation of non-aromatic volatile organic compounds. Atmos. Chem. Phys. 3, 161–180.

Selin, N.E., Wu, S., Nam, K.M., Reilly, J.M., Paltsev, S., Prinn, R.G., Webster, M.D., 2009. Global health and economic impacts of future ozone pollution. Environ. Res. Lett. 4, 9.

Sillman, S., 1999. The relation between ozone, $NO_x$ and hydrocarbons in urban and polluted rural environments. Atmos. Environ. 33, 1821–1845.

Sun, L., Xue, L.K., Wang, T., Gao, J., Ding, A.J., Cooper, O.R., Lin, M.Y., Xu, P.J., Wang, Z., Wang, X.F., Wen, L., Zhu, Y.H., Chen, T.S., Yang, L.X., Wang, Y., Chen, J.M., Wang, W.X., 2016. Significant increase of summertime ozone at mount tai in central eastern China. Atmos. Chem. Phys. 16, 10637–10650.

Sun, L., Xue, L., Wang, Y., Li, L., Lin, J., Ni, R., Yan, Y., Chen, L., Li, J., Zhang, Q., 2019. Impacts of meteorology and emissions on summertime surface ozone increases over central eastern China between 2003 and 2015. Atmos. Chem. Phys. 19, 1455–1469.

Tang, G., Wang, Y., Li, X., Ji, D., Hsu, S., Gao, X., 2012. Spatial-temporal variations in surface ozone in Northern China as observed during 2009-2010 and possible implications for future air quality control strategies. Atmos. Chem. Phys. 12, 2757–2776.

Wang, T., Wei, X.L., Ding, A.J., Poon, C.N., Lam, K.S., Li, Y.S., Chan, L.Y., Anson, M., 2009. Increasing surface ozone concentrations in the background atmosphere of Southern China, 1994-2007. Atmos. Chem. Phys. 9, 6217–6227.

Wang, T., Xue, L.K., Brimblecombe, P., Lam, Y.F., Li, L., Zhang, L., 2017. Ozone pollution in China: A review of concentrations, meteorological influences, chemical precursors, and effects. Sci. Total Environ. 575, 1582–1596.

Wang, T., Xue, L., Feng, Z., Dai, J., Zhang, Y., Tan, Y., 2022. Ground-level ozone pollution in China: a synthesis of recent findings on influencing factors and impacts. Environ. Res. Lett. 17, 063003.

Wang, Y., Guo, H., Zou, S.C., Lyu, X.P., Ling, Z.H., Cheng, H.R., Zeren, Y.Z., 2018. Surface $O_3$ photochemistry over the South China Sea: application of a near-explicit chemical mechanism box model. Environ. Pollut. 234, 155–166.

Xue, L.K., Wang, T., Gao, J., Ding, A.J., Zhou, X.H., Blake, D.R., Wang, X.F., Saunders, S.M., Fan, S.J., Zuo, H.C., Zhang, Q.Z., Wang, W.X., 2014a. Ground-level ozone in four Chinese cities: precursors, regional transport and heterogeneous processes. Atmos. Chem. Phys. 14, 13175–13188.

Xue, L.K., Gu, R.R., Wang, T., Wang, X.F., Saunders, S., Blake, D., Louie, P.K.K., Luk, C.W.Y., Simpson, I., Xu, Z., Wang, Z., Gao, Y., Lee, S.C., Mellouki, A., Wang, W.X., 2016. Oxidative capacity and radical chemistry in the polluted atmosphere of Hong Kong and Pearl River Delta region: analysis of a severe photochemical smog episode. Atmos. Chem. Phys. 16, 9891–9903.

Xue, L.K., Wang, T., Louie, P.K.K., Luk, C.W.Y., Blake, D.R., Xu, Z., 2014b. Increasing external effects negate local efforts to control ozone air pollution: a case study of Hong Kong and implications for other Chinese cities. Environ. Sci. Technol. 48, 10769–10775.

Yang, W.Y., Chen, H.S., Wang, W.D., Wu, J.B., Li, J., Wang, Z.F., Zheng, J.Y., Chen, D.H., 2019. Modeling study of ozone source apportionment over the Pearl River Delta in 2015. Environ. Pollut. 253, 393–402.

Zeng, Y.Y., Cao, Y.F., Qiao, X., Seyler, B.C., Tang, Y., 2019. Air pollution reduction in China: recent success but great challenge for the future. Sci. Total Environ. 663, 329–337.

Zhang, Y.N., Sun, J.J., Zheng, P.G., Chen, T.S., Liu, Y.H., Han, G.X., Simpson, I.J., Wang, X.F., Blake, D.R., Li, Z.Y., Yang, X., Qi, Y.B., Wang, Q., Wang, W.X., Xue, L.K., 2019. Observations of $C_1$-$C_5$ alkyl nitrates in the Yellow River Delta, northern China: effects of biomass burning and oil field emissions. Sci. Total Environ. 656, 129–139.

Zhang, Y.N., Xue, L.K., Carter, W.P.L., Pei, C.L., Chen, T.S., Mu, J.S., Wang, Y.J., Zhang, Q.Z., Wang, W.X., 2021. Development of ozone reactivity scales for volatile organic compounds in a Chinese megacity. Atmos. Chem. Phys. 21, 11053–11068.

Zhao, H., Chen, K., Liu, Z., Zhang, Y., Shao, T., Zhang, H., 2021. Coordinated control of $PM_{2.5}$ and $O_3$ is urgently needed in China after implementation of the "Air pollution prevention and control action plan". Chemosphere 270, 129441.

Zheng, J., Zhong, L., Wang, T., Louie, P.K.K., Li, Z., 2010. Ground-level ozone in the Pearl River Delta region: analysis of data from a recently established regional air quality monitoring network. Atmos. Environ. 44, 814–823.

Zong, R.H., Xue, L.K., Wang, T.B., Wang, W.X., 2018. Inter-comparison of the regional atmospheric chemistry mechanism (RACM2) and master chemical mechanism (MCM) on the simulation of acetaldehyde. Atmos. Environ. 186, 144–149.